

Heisenberg-limited spin squeezing in coupled spin systems

Long-Gang Huang^{1,*}, Xuanchen Zhang^{1,*}, Yanzhen Wang^{1,*}, Zhenxing Hua¹, Yuanjiang Tang¹, and Yong-Chun Liu^{1,2†}

¹*State Key Laboratory of Low-Dimensional Quantum Physics,*

Department of Physics, Tsinghua University, Beijing 100084, P. R. China and

²*Frontier Science Center for Quantum Information, Beijing 100084, P.R. China*

(Dated: March 27, 2023)

Spin squeezing plays a crucial role in quantum metrology and quantum information science. Its generation is the prerequisite for further applications but still faces an enormous challenge since the existing physical systems rarely contain the required squeezing interactions. Here we propose a universal scheme to generate spin squeezing in coupled spin models with collective spin-spin interactions, which commonly exist in various systems. Our scheme can transform the coupled spin interactions into squeezing interactions, and reach the extreme squeezing with Heisenberg-limited measurement precision scaling as $1/N$ for N particles. Only constant and continuous driving fields are required, which is accessible to a series of current realistic experiments. This work greatly enriches the variety of systems that can generate the Heisenberg-limited spin squeezing, with broad applications in quantum precision measurement.

I. INTRODUCTION

Squeezed spin states (SSSs) are entangled quantum states of collective spins with reduced quantum fluctuations in one spin component perpendicular to the mean spin direction, due to the quantum correlation between spins [1–4]. The reduced quantum fluctuations allow them to surpass the so-called standard quantum limit (SQL) with measurement precision scales as $\propto 1/N^{1/2}$ for N particles [5–9], which is permitted by the coherent spin states (CSSs). Thereby, the SSSs are the key resources in the field of quantum metrology, which have significant applications in high-precision measurements [2, 3, 10–21]. Due to their close relationship with quantum correlation, they also serve as a significant witness to reveal the many-particle entanglement, which have attracted extensive research interests during the past few decades [22–33]. Since their preparation is the prerequisite for further applications, many efforts have been made to produce the SSSs, mainly in two categories of platforms: atom-light interactions [15, 34–42] and nonlinear atom-atom interactions, e.g., Bose-Einstein condensates (BECs) [13, 14, 22, 27, 43, 44].

Among the category of atom-light interaction platform, one method of generating spin squeezing is by transferring the squeezing from squeezed light to spin system [34, 45–47]. It is straightforward but limited by the transfer efficiency and the performance of light squeezing. Besides, some proposals use photon-mediated spin-spin interactions generated in an optical cavity to obtain SSSs [48, 49], in which case superradiance is the main restriction on the achievable squeezing. Quantum non-demolition (QND) measurement is another experimentally feasible way to generate spin squeezing [7, 50–54], but the acquired squeezing is not deterministic and there-

fore strongly depends on the performance of the photodetector [18, 55]. For the nonlinear atom-atom interaction platform, two well-known mechanisms, i.e., one-axis twisting (OAT) and two-axis twisting (TAT) can deterministically generate the spin squeezing [1, 4, 56–61]. Interparticle interactions in BEC lead to OAT dynamics in certain circumstances, which has been realized in several experiments to create metrologically useful squeezing [13, 14]. Studies in trapped ions [31, 62, 63] and superconducting qubits [64–66] also witness OAT interaction and use it for entanglement generation. Though the OAT squeezing has been experimentally demonstrated in these systems, the squeezing degree only scales as $\propto 1/N^{2/3}$, which is still far from the Heisenberg-limited measurement precision. In contrast, the TAT squeezing can provide a fascinating squeezing degree scaling as $\propto 1/N$, which can reach the Heisenberg-limit measurement precision, but its generation remains a great challenge since the interaction form is not found naturally in current realistic physical systems [40, 56–61, 67–70]. For certain existing interactions with weak or without squeezing ability, utilization of pulse sequences is shown to possibly induce engineered OAT or TAT Hamiltonian [71–75]. Several other theoretical schemes are devoted to transforming the OAT interaction into a TAT type to approach the ultimate Heisenberg limit [56–59, 61]. However, either special experimental systems or complicated designs are required in these proposals. Therefore, it is essential to explore feasible schemes capable of realizing Heisenberg-limited squeezing with commonly-existed systems and easily-implementable designs.

Here we propose a universal scheme to produce Heisenberg-limited spin squeezing in generic coupled spin systems with collective spin-spin interactions by continuous drivings. An effective OAT interaction can be induced by simply applying a constant direct-current (DC) field, leading to strong spin squeezing. We can further obtain the TAT spin squeezing with an additional continuous alternating-current (AC) field, and the Heisenberg-limited measurement precision is ultimately achieved.

* These authors contributed equally to this work.

† ycliu@tsinghua.edu.cn

Unlike schemes such as those reported in Ref. [76] and Ref. [77], which require an intrinsic spin-squeezing interaction that can be enhanced through drives, our scheme focuses on generating spin squeezing from a collective interaction that does not intrinsically result in spin squeezing. As a result, our scheme largely enriches the variety of systems that can realize or enhance spin squeezing. Meanwhile, unlike previous studies, our approach only needs a constant field to generate effective OAT interaction and an additional continuous driving to generate effective TAT interaction, which is favorable for experimental implementation.

II. SYSTEM MODEL

A broad category of coupled spin systems can be universally described by the collective interaction Hamiltonian

$$H_{\text{int}} = \sum_{\mu} g_{\mu} S_{\mu} J_{\mu}, \quad (1)$$

where g_{μ} ($\mu = x, y, z$) denotes the coupling strength between the two subsystems for different spin components, described by the collective spins (or pseudospins) \mathbf{S} and \mathbf{J} , respectively. The operators are defined as $S_{\mu} = \sum_{k=1}^{N_s} \sigma_{S,\mu}^{(k)}/2$ and $J_{\mu} = \sum_{k=1}^{N_j} \sigma_{J,\mu}^{(k)}/2$, denoting the collective spin components, with $\sigma_{S,\mu}^{(k)}$ and $\sigma_{J,\mu}^{(k)}$ being the corresponding Pauli matrices for the k -th spin-1/2 (or two-level) particle. They can also describe the Stokes operators of light, which are related to the differences between the number operators of the photons polarized in different orthogonal bases [4, 18]. The operators satisfy the SU(2) angular momentum commutation relations $[S_i, S_j] = i\varepsilon_{ijk} S_k$ and $[J_i, J_j] = i\varepsilon_{ijk} J_k$, where ε_{ijk} ($i, j, k = x, y, z$) is the Levi-Civita symbol. The above model can be used to describe the atom-light interaction system [9, 55], spin-exchange interaction system, dipole-dipole interaction system, etc. The corresponding typical interaction Hamiltonians are $H_1 = gS_z J_z$, $H_2 = g(S_x J_x + S_y J_y + S_z J_z)$ and $H_3 = g(S_x J_x + S_y J_y - 2S_z J_z)$, as illustrated in Fig. 1(a), (b) and (c), respectively.

Considering the practical applications, we focus on the spin squeezing of one subsystem, e.g., spin S . The interaction Hamiltonian (1) does not contain the intra-species nonlinear interaction form like S_{μ}^2 , thus not being able to generate the OAT interactions. We apply constant DC driving fields on both subsystems, generally described by

$$H_{\text{driv}}^{\text{DC}} = \Omega J_z + \Omega' S_z. \quad (2)$$

Here Ω and Ω' denote the magnitudes of homogeneous fields along z axis applied on spins S and J , respectively. Thereby, the total Hamiltonian becomes $H_{\text{tot}} = H_{\text{int}} + H_{\text{driv}}^{\text{DC}}$, which will be demonstrated to be equivalent to an effective OAT form $\propto S_z^2$ in the following.

To be specific, the mechanism of inducing OAT spin squeezing is analogous to that of electron-phonon interaction in condensed matter physics, in which the effective

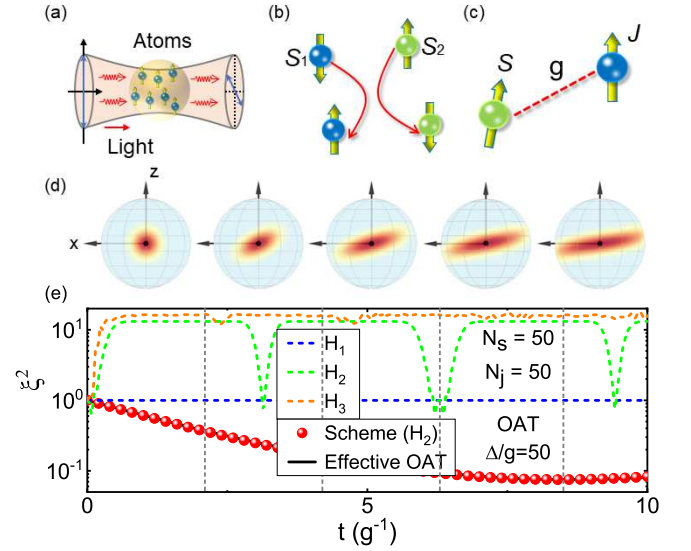


FIG. 1. Schematic diagram of coupled spin systems and spin squeezing via constant drivings. (a) Schematic diagram of atom-light interaction system with Faraday magneto-optic rotation. (b) Schematic diagram of spin-exchange interaction between two spins. (c) Schematic diagram of dipole-dipole interaction between two spins. (d) Evolution of the quantum state for spin S at the time instants denoted by the vertical gray dashed lines in (e), represented by the Husimi Q function on the generalized Bloch spheres. (e) The blue dashed line, green and orange dashed curves respectively present the free evolution of the squeezing parameters ξ^2 for spin S under the Hamiltonians H_1 , H_2 and H_3 as defined in the main text. The red solid balls denote the results of our scheme with H_2 under constant drivings, compared with the effective OAT interaction (5) (black solid curve). The vertical gray dashed lines mark time instants of $t = t_{\text{min}}/4$, $t_{\text{min}}/2$, $3t_{\text{min}}/4$ and t_{min} , with t_{min} being the optimal squeezing time of OAT. The parameters are $N_s = 50$, $N_j = 50$ and $\Delta/g = 50$. The initial state is product of coherent spin states polarized along y axis for spin S and z axis for spin J .

electron-electron interaction is mediated by the phonons (lattice vibrations). In our scheme, the spin J acts as an intermediary (analogous to the role of phonons) to induce the intra-species interaction in the spin S (analogous to the role of electrons). The effective intra-species interaction in spin S can be derived by performing the Fröhlich-Nakajima transformation (FNT) [78, 79] with $U = e^S$ on the total Hamiltonian of the coupled spin system as

$$H_{\text{eff}} = e^{-S} H_{\text{tot}} e^S = H_{\text{driv}}^{\text{DC}} + (H_{\text{int}} + [H_{\text{driv}}^{\text{DC}}, S]) + \frac{1}{2} [(H_{\text{int}} + [H_{\text{driv}}^{\text{DC}}, S]), S] + \frac{1}{2} [H_{\text{int}}, S] + \dots, \quad (3)$$

Choosing an appropriate $S = -i\theta_{xy} S_x J_y - i\theta_{yx} S_y J_x$ with θ_{xy} and θ_{yx} being undetermined coefficients, so that the first order term $H_{\text{int}} + [H_{\text{driv}}^{\text{DC}}, S]$ almost vanishes, the Hamiltonian is simplified as $H_{\text{eff}} \simeq H_{\text{driv}}^{\text{DC}} + [H_{\text{int}}, S]/2$. The commutator $[H_{\text{int}}, S]$ contains the quadratic terms

S_μ^2 , thus being able to generate the OAT spin squeezing (see Appendix A for detailed derivations).

Furthermore, the initial state of spin J is chosen to be a CSS polarized along z axis, i.e., the eigenstate of J_z with eigenvalue $N_j/2$, where N_j is the corresponding particle number. During short time evolution, the operators describing the spin J can be approximately replaced by their expectation values in the initial state. As a result, the Hamiltonian becomes

$$H_{\text{eff}} = fS_z + pS_x^2 + qS_y^2, \quad (4)$$

where f, p, q are functions of Ω and Ω' (see Appendix A). Appropriate combination of Ω and Ω' can make $f = 0$, eliminating the linear term in Eq. (4). When $p = q$ (the case is similar when one of p and q is 0), Eq. (4) is reduced to a pure OAT Hamiltonian

$$H_{\text{eff}}^{\text{OAT}} = \chi_{\text{eff}} S_z^2, \quad (5)$$

with the effective nonlinear interaction strength $\chi_{\text{eff}} = -g^2/(2\Delta)$. Here $\Delta = 2(\Omega - \Omega')/(N_j)$ is a parameter characterizing the difference between the magnitudes of two external fields. The condition $p = q$ can be satisfied when $g_x = g_y \equiv g$. Note that the sign and magnitude of the interaction strength χ_{eff} can be easily modulated by adjusting the magnitudes of fields Ω and Ω' , which allows our scheme to be directly applied in the twisting echo protocol proposed in Ref. [80, 81] that is robust against detection noise.

III. NUMERICAL INVESTIGATION OF SQUEEZING DYNAMICS

Now we investigate the evolutions of the quantum state with constant drivings. Demonstrated by Husimi Q representation on the generalized Bloch spheres, the isotropic variance of the initial CSS of spin S is continuously redistributed and reduced in a certain direction, indicating the spin squeezing, as is shown in Fig. 1(d). The degree of spin squeezing is usually quantified by the squeezing parameter $\xi^2 = 4(\Delta S_\perp)_{\text{min}}^2/N_s$ [1], where $(\Delta S_\perp)_{\text{min}}^2$ is the minimum of the fluctuation $(\Delta S_\perp)^2 = \langle S_\perp^2 \rangle - \langle S_\perp \rangle^2$ for the spin component perpendicular to the mean spin direction. We compare the squeezing parameters for free evolution under the three Hamiltonians H_1, H_2, H_3 , and for the evolution of H_2 with constant drivings, as shown in Fig. 1(e). It clearly shows that our scheme largely improves the squeezing properties. Note that applying constant drivings on Hamiltonians H_1 and H_3 would also lead to the improvement to the OAT squeezing.

According to the previous conclusion of OAT squeezing [82] and based on the obtained effective interaction coefficient χ_{eff} , we derive the optimal spin squeezing parameter and the corresponding squeezing time as

$$\xi_{\text{min}}^2 \simeq \frac{1}{2} \left(\frac{N_s}{3} \right)^{-\frac{2}{3}}, \quad t_{\text{min}} \simeq \frac{2 \times 3^{1/6} \Delta}{g^2 N_s^{2/3}}. \quad (6)$$

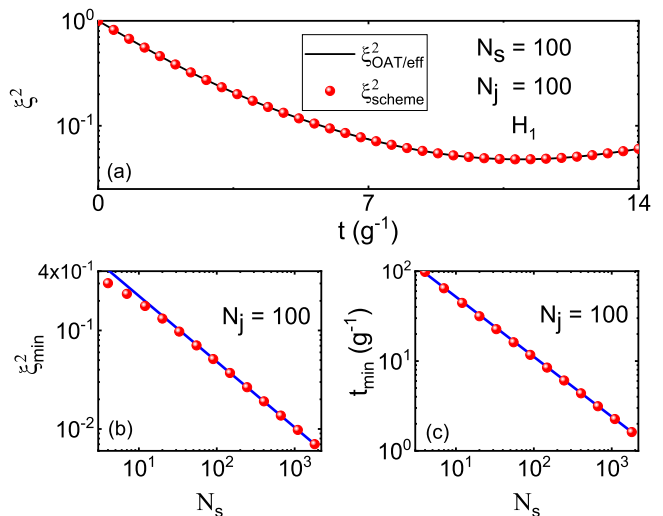


FIG. 2. The effective OAT spin squeezing under Hamiltonian H_1 with constant DC driving field. (a) Evolution of the spin squeezing parameter ξ^2 of our scheme with constant drivings (red solid balls), compared with that of the corresponding effective OAT Hamiltonian (5) (black solid curve). (b) and (c) demonstrate the optimal spin squeezing parameter ξ_{min}^2 and the corresponding squeezing time t_{min} as functions of particle number N_s (red solid balls). The blue solid lines are predicted by equation (6). The parameter $\Omega = 50N_j g$ with particle numbers given in each subgraph.

The validity of effective OAT squeezing is further demonstrated in Fig. 2. The evolution of the squeezing parameter with constant drivings agrees well with the corresponding effective OAT Hamiltonian (5), as is shown in Fig. 2(a). The power-law scalings given in Eq. (6) are also verified in Fig. 2(b) and (c).

Although Eq. (4) shows that both S_x^2 and S_y^2 exist, the tuning ranges of parameters p and q are not broad enough to directly obtain the effective TAT interaction with the form $\propto (S_i^2 - S_j^2)$. This imperfection can be overcome by adding an additional continuous AC driving field, e.g., $H_{\text{driv}}^{\text{AC}} = A \cos(\omega t) S_z$, with A and ω being the amplitude and frequency of the driving field, respectively. The total driving terms including $H_{\text{driv}}^{\text{DC}}$ and $H_{\text{driv}}^{\text{AC}}$ become

$$H_{\text{driv}} = \Omega J_z + \Omega' S_z + A \cos(\omega t) S_z, \quad (7)$$

and the total Hamiltonian then becomes $H'_{\text{tot}} = H_{\text{int}} + H_{\text{dirv}}$. Now we apply two transformations on the total Hamiltonian, one is the same FNT as described by Eq. (3), the other is $U_I(t) = \exp[-i \int_0^t H_{\text{driv}}^{\text{AC}}(\tau) d\tau]$. Then the Hamiltonian can be simplified as $H_I \simeq [(p+q)/2 - (q-p)J_0(2A/\omega)/2]S_x^2 + [(p+q)/2 + (q-p)J_0(2A/\omega)/2]S_y^2$, where $J_n(z)$ is the n -th Bessel function of the first kind. Therefore, when A/ω is properly chosen, H_I will be a TAT Hamiltonian under the condition $(p-2q)(2p-q) \geq 0$. For other cases, e.g., $p = q$, the continuous AC driving field can be applied along the y direction with $H_{\text{driv}}^{\text{AC}} =$

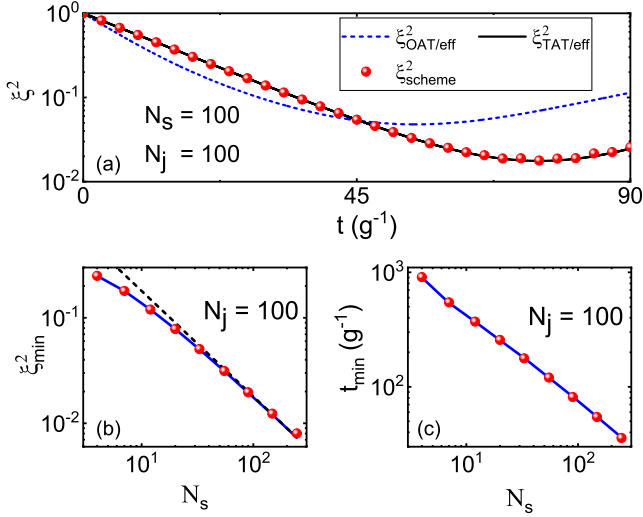


FIG. 3. The effective TAT spin squeezing under Hamiltonian H_2 with DC and AC driving fields. (a) Evolution of the spin squeezing parameter ξ^2 for coupled spin systems with drivings (red solid balls) and for the effective TAT Hamiltonian (8) (black solid curve), compared with the OAT spin squeezing (blue dashed curve) governed by Hamiltonian (5). (b) and (c): The optimal spin squeezing ξ_{\min}^2 and the optimal squeezing time t_{\min} as functions of the particle number N_s for the TAT scheme with drivings (red solid balls), compared with the effective TAT results (blue solid curves). The black dashed line in (b) corresponds to $\xi_{\min}^2 = 1.8/N_s$. The parameter $\Delta/g = 100$ and particle numbers are given in each subgraph.

A $\cos(\omega t)S_y$, which yields

$$H_{\text{eff}}^{\text{TAT}} = \frac{\chi_{\text{eff}}}{3}(S_x^2 - S_y^2), \quad (8)$$

where χ_{eff} is the same as the OAT case (see Appendix B for detailed derivations).

To verify the validity of our TAT scheme, we numerically study the evolution of spin squeezing parameter of Hamiltonian (1), coupled with the total driving (7), compared with the effective TAT Hamiltonian (8). As is shown in Fig. 3(a), the evolution of spin squeezing parameter under our scheme agrees well with that of the effective TAT Hamiltonian dynamics, performing much better than the OAT spin squeezing. As the effective interaction strength of TAT spin squeezing is obtained in Eq. (8) ($\chi_{\text{eff}}/3$), the power-law scalings can be approximately obtained according to the standard TAT squeezing [56]

$$\xi_{\min}^2 \simeq \frac{1.8}{N_s}, \quad t_{\min} \simeq \frac{3\Delta \ln(4N_s)}{g^2 N_s}. \quad (9)$$

They are also verified in Fig. 3(b) and (c). Therefore, adding both DC and AC driving fields will finally transform the initial interaction (1) into the TAT interaction, with squeezing degree up to the Heisenberg-limited measurement precision.

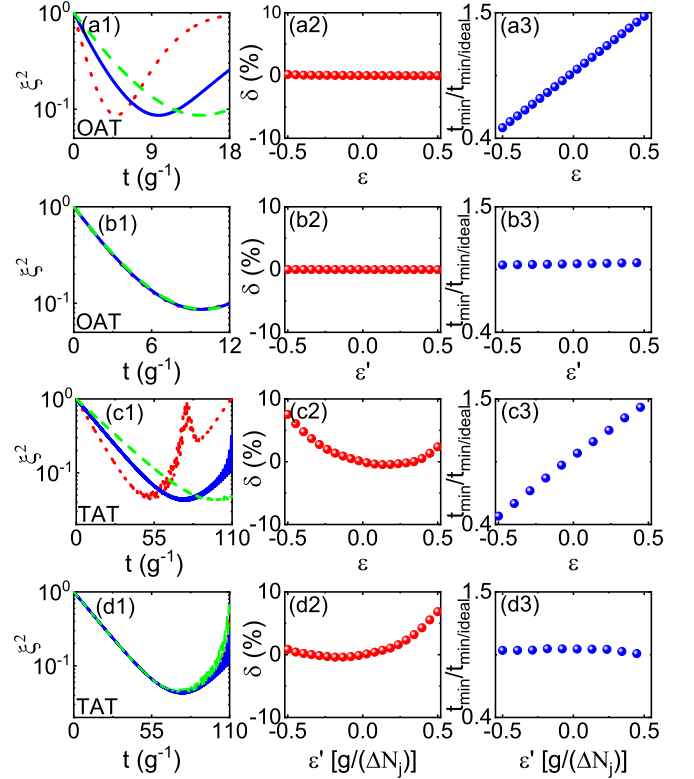


FIG. 4. The influence of parameter imperfections. The first row (a1-a3) show the effective OAT spin squeezing under different deviations of Ω , denoted as ϵ . The second row (b1-b3) are the results for the deviation of Ω' , denoted as ϵ' . The third (c1-c3) and fourth (d1-d3) rows are the corresponding results of the effective TAT spin squeezing under different ϵ and ϵ' , respectively. The deviations ϵ , ϵ' and relative error δ are defined in the main text. For the first column (a1-d1), the dotted red, solid blue, dashed green curves correspond to (a1) $\epsilon = -0.5, 0, 0.5$, (b1) $\epsilon' = -1, 0, 1$, (c1) $\epsilon = -0.3, 0, 0.3$ and (d1) $\epsilon' = -2 \times 10^{-5}, 0, 2 \times 10^{-5}$, respectively. The parameters are $\Delta/g = 50$ for OAT and $\Delta/g = 250$ for TAT spin squeezing, and the particle numbers are $N_s = N_j = 40$.

IV. DISCUSSION ON PARAMETER IMPERFECTIONS

Considering the realistic experimental system, we investigate the influence of parameter imperfections. On one hand, during the derivation of effective interaction, the magnitudes of Ω and Ω' should satisfy the constraint $f = 0$ in order to eliminate the linear term in the effective Hamiltonian. Here we investigate the influence of the deviation of Ω or Ω' from their ideal values, keeping the value of the other one unchanged. The deviations are quantified by the relative error, defined as $\epsilon = (\Omega - \Omega_{\text{ideal}})/\Omega_{\text{ideal}}$ for Ω and $\epsilon' = (\Omega' - \Omega'_{\text{ideal}})/\Omega'_{\text{ideal}}$ for Ω' , respectively. As shown in Fig. 4(a1)-(d1) (the first column), the evolutions of the spin squeezing parameters ξ^2 deviate from the ideal cases to some extent, but the squeezing is not much degraded. The optimal squeez-

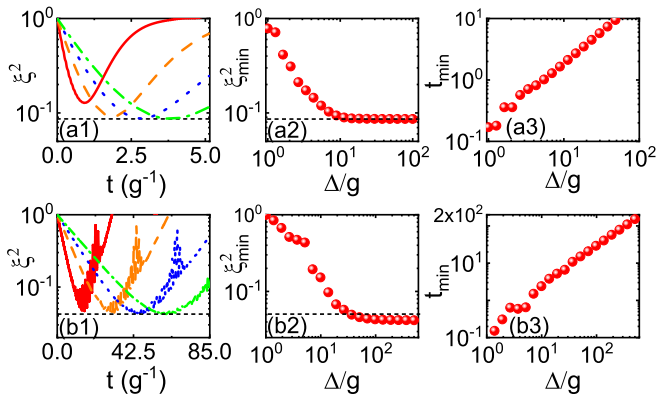


FIG. 5. Spin squeezing under different Δ . The top panel (a1-a3) demonstrates the evolution of spin squeezing parameter ξ^2 under different Δ , the optimal spin squeezing ξ_{\min}^2 and the optimal squeezing time t_{\min} as functions of Δ , for the OAT spin squeezing. The bottom panel (b1-b3) show the results for the TAT spin squeezing. For the first column (a1-b1), the solid red, dashed orange, dotted blue, dash-dotted green curves correspond to (a1) $\Delta/g = 5, 10, 15, 20$ and (a2) $\Delta/g = 50, 100, 150, 200$, respectively. The horizontal dashed lines denote the optimal spin squeezing achieved by a standard OAT squeezing in (a1-a2) and a standard TAT one in (b1-b2). The particle numbers are $N_s = N_j = 40$.

ing is insensitive to the deviations for OAT while slightly sensitive for TAT squeezing, as shown in Fig. 4(a2)-(d2) (the second column) with the relative error of optimal squeezing parameter $\delta = (\xi_{\min}^2 - \xi_{\min 0}^2)/\xi_{\min 0}^2$. This is due to the fact that the effective TAT squeezing needs the rotation of twisting axis, which is susceptible to the linear term in the total Hamiltonian. Nevertheless, it still stays within the relative error of 10% for relatively large deviations, as shown in Fig. 4(c2)-(d2). Therefore, our scheme is overall robust to the deviation from the ideal combination of Ω and Ω' . The optimal squeezing times t_{\min} increase linearly as the deviation of Ω increases, but are not sensitive to the deviation of Ω' . This is because χ_{eff} is in inverse proportional to $\Delta \propto (\Omega - \Omega')$, and Ω is assumed to be much larger than Ω' in the plots.

On the other hand, we investigate the influence of Δ on the effective spin squeezing, as is shown in Fig. 5. Overall, the best attainable squeezing ξ_{\min}^2 becomes better with the increase of Δ [Fig. 5(a2) and (b2)], while the optimal squeezing time t_{\min} also increases [Fig. 5(a3) and (b3)]. Specifically, given the particle numbers, when the value of Δ is larger than a certain value, the best attainable spin squeezing can achieve the optimal spin squeezing for the corresponding effective OAT or TAT spin squeezing, as shown in Fig. 5(a2) and (b2). Approximately, it requires $\Delta/g \gg 10$ for OAT squeezing and $\Delta/g \gg 50$ for TAT squeezing, which shows that the condition for realizing TAT squeezing is relatively stringent than that of OAT, and the required squeezing time seems to be longer. Nevertheless, the above discussions are limited by the particle numbers due to the constrain of numerical computation resources. Since the optimal squeezing

time t_{\min} scales as $\ln(4N_s)/N_s$ for TAT squeezing, for very large N_s , the required squeezing time will not need to be too long.

V. CONCLUSION

In summary, we have proposed a universal scheme to generate the effective OAT and TAT spin squeezing in a broad category of coupled spin systems with collective interaction Hamiltonian $H_{\text{int}} = \sum_{\mu} g_{\mu} S_{\mu} J_{\mu}$, by applying only constant and continuous drivings, which are simple to implement. Both the best attainable spin squeezing and the corresponding optimal time as functions of particle number are demonstrated to satisfy the power-law scalings of OAT or TAT squeezing. In particular, Heisenberg-limited measurement precision can be reached in such coupled spin systems. Furthermore, our scheme is demonstrated to be tolerant to the parameter imperfections of the driving fields. This work offers the opportunity to realize Heisenberg-limited spin squeezing in a variety of coupled spin systems that are common in realistic physical systems.

ACKNOWLEDGMENTS

This work is supported by the Key-Area Research and Development Program of Guangdong Province (Grant No. 2019B030330001), the National Natural Science Foundation of China (NSFC) (Grant Nos. 12275145, 92050110, 91736106, 11674390, and 91836302), and the National Key R&D Program of China (Grants No. 2018YFA0306504).

Appendix A: Derivation of the effective squeezing Hamiltonian

Starting from the total Hamiltonian

$$H_{\text{tot}} = \Omega J_z + \Omega' S_z + \sum_{\mu} g_{\mu} S_{\mu} J_{\mu}, \quad (\text{A1})$$

we perform the Fröhlich-Nakajima transformation (FNT) to obtain the squeezing Hamiltonian.

To be specific, we introduce a unitary transformation

$$U = e^S, \quad (\text{A2})$$

where

$$S = -i(\theta_{xy} S_x J_y + \theta_{yx} S_y J_x). \quad (\text{A3})$$

The Hamiltonian is then transformed into

$$\begin{aligned} H' &= e^{-S} H_{\text{tot}} e^S \\ &= H_{\text{tot}} + [H_{\text{tot}}, S] + \frac{1}{2} [[H_{\text{tot}}, S], S] + \dots \end{aligned} \quad (\text{A4})$$

We calculate the commutator $[H_{\text{tot}}, S]$ as

$$\begin{aligned}
[H_{\text{tot}}, S] &= \Omega[J_z, -i(\theta_{xy}S_xJ_y + \theta_{yx}S_yJ_x)] + \Omega'[S_z, -i(\theta_{xy}S_xJ_y + \theta_{yx}S_yJ_x)] \\
&\quad + [g_xS_xJ_x + g_yS_yJ_y + g_zS_zJ_z, -i(\theta_{xy}S_xJ_y + \theta_{yx}S_yJ_x)] \\
&= -(\theta_{xy}\Omega + \theta_{yx}\Omega')S_xJ_x + (\theta_{yx} + \theta_{xy}\Omega')S_yJ_y + g_x\theta_{xy}S_x^2J_z - g_y\theta_{yx}S_y^2J_z \\
&\quad + g_x\theta_{yx}S_zJ_x^2 - g_y\theta_{xy}S_zJ_y^2 + g_z\theta_{xy}(-S_zS_xJ_x + S_yJ_yJ_z) + g_z\theta_{yx}(S_zS_yJ_y - S_xJ_xJ_z),
\end{aligned} \tag{A5}$$

and further obtain

$$\begin{aligned}
[[H_{\text{tot}}, S], S] &= -(\theta_{xy}\Omega + \theta_{yx}\Omega')\theta_{xy}S_x^2[J_x, -iJ_y] + (\theta_{yx}\Omega + \theta_{xy}\Omega')\theta_{xy}[S_y, -iS_x]J_y^2 \\
&\quad - (\theta_{xy}\Omega + \theta_{yx}\Omega')\theta_{yx}[S_x, -iS_y]J_x^2 + (\theta_{yx}\Omega + \theta_{xy}\Omega')\theta_{yx}S_y^2[J_y, -iJ_x] + \dots \\
&= -(\theta_{xy}\Omega + \theta_{yx}\Omega')\theta_{xy}S_x^2J_z - (\theta_{yx}\Omega + \theta_{xy}\Omega')\theta_{xy}S_zJ_y^2 \\
&\quad - (\theta_{xy}\Omega + \theta_{yx}\Omega')\theta_{yx}S_zJ_x^2 - (\theta_{yx}\Omega + \theta_{xy}\Omega')\theta_{yx}S_y^2J_z + \dots
\end{aligned} \tag{A6}$$

Replace them into (A4), we get

$$\begin{aligned}
H' &= \Omega J_z + \Omega' S_z + (g_x - \theta_{xy}\Omega - \theta_{yx}\Omega')S_xJ_x + (g_y + \theta_{yx}\Omega + \theta_{xy}\Omega')S_yJ_y + g_zS_zJ_z \\
&\quad + \left[g_x - \frac{1}{2}(\theta_{xy}\Omega + \theta_{yx}\Omega') \right] \theta_{xy}S_x^2J_z - \left[g_y + \frac{1}{2}(\theta_{yx}\Omega + \theta_{xy}\Omega') \right] S_y^2J_z \\
&\quad + \left[g_x - \frac{1}{2}(\theta_{xy}\Omega + \theta_{yx}\Omega') \right] \theta_{yx}S_zJ_x^2 - \left[g_y + \frac{1}{2}(\theta_{yx}\Omega + \theta_{xy}\Omega') \right] S_zJ_y^2 \\
&\quad + g_z\theta_{xy}(-S_zS_xJ_x + S_yJ_yJ_z) + g_z\theta_{yx}(S_zS_yJ_y - S_xJ_xJ_z) + \dots
\end{aligned} \tag{A7}$$

In the spirit of FNT, we require

$$\begin{aligned}
g_x - \theta_{xy}\Omega - \theta_{yx}\Omega' &= 0, \\
g_y + \theta_{yx}\Omega + \theta_{xy}\Omega' &= 0,
\end{aligned} \tag{A8}$$

which leads to

$$\theta_{xy} = \frac{g_x\Omega + g_y\Omega'}{\Omega^2 - \Omega'^2}, \quad \theta_{yx} = -\frac{g_y\Omega + g_x\Omega'}{\Omega^2 - \Omega'^2}. \tag{A9}$$

The expression of H' now becomes

$$\begin{aligned}
H' &= \Omega J_z + \Omega' S_z + g_zS_zJ_z + \frac{g_x^2\Omega + g_xg_y\Omega'}{2(\Omega^2 - \Omega'^2)}S_x^2J_z + \frac{g_y^2\Omega + g_xg_y\Omega'}{2(\Omega^2 - \Omega'^2)}S_y^2J_z - \frac{g_x^2\Omega' + g_xg_y\Omega}{2(\Omega^2 - \Omega'^2)}S_zJ_x^2 \\
&\quad - \frac{g_y^2\Omega' + g_xg_y\Omega}{2(\Omega^2 - \Omega'^2)}S_zJ_y^2 + \frac{g_xg_z\Omega + g_yg_z\Omega'}{\Omega^2 - \Omega'^2}(-S_zS_xJ_x + S_yJ_yJ_z) - \frac{g_yg_z\Omega + g_xg_z\Omega'}{\Omega^2 - \Omega'^2}(S_zS_yJ_y - S_xJ_xJ_z) + \dots
\end{aligned} \tag{A10}$$

In order to ignore higher order terms safely, the derivations above require

$$\frac{gN_s}{|\Omega - \Omega'|} \ll 1 \quad \& \quad \frac{gN_j}{|\Omega - \Omega'|} \ll 1. \tag{A11}$$

When focusing on the evolution of subsystem \mathbf{S} , we choose the initial state of subsystem \mathbf{J} as the coherent spin state along $+z$ axis, i.e., $|\psi(t=0)\rangle_{\mathbf{J}} = |z\rangle$, and as-

sume it is almost unchanged during evolution. Then we can replace the operators of subsystem \mathbf{J} with their expected values:

$$\begin{aligned}
\langle J_z \rangle &= \frac{N_j}{2}, \quad \langle J_x^2 \rangle = \langle J_y^2 \rangle = \frac{N_j}{4}, \\
\langle J_x \rangle &= \langle J_y \rangle = \langle J_zJ_y \rangle = \langle J_zJ_x \rangle = 0.
\end{aligned} \tag{A12}$$

After that, we finally obtain the effective Hamiltonian for

the subsystem **S**:

$$H_{\text{eff}} = fS_z + pS_x^2 + qS_y^2, \quad (\text{A13})$$

where

$$f = \Omega' + \frac{1}{2}g_z N_j - \frac{N_j}{8(\Omega^2 - \Omega'^2)} [(g_x^2 + g_y^2)\Omega' + 2g_x g_y \Omega],$$

$$p = \frac{N_j(g_x^2 \Omega + g_x g_y \Omega')}{4(\Omega^2 - \Omega'^2)}, \quad q = \frac{N_j(g_y^2 \Omega + g_x g_y \Omega')}{4(\Omega^2 - \Omega'^2)}. \quad (\text{A14})$$

For three typical interactions $H_1 = gS_x J_x$, $H_2 = g(S_x J_x + S_y J_y + S_z J_z)$, $H_3 = g(S_x J_x + S_y J_y - 2S_z J_z)$, the corresponding effective Hamiltonians are

$$H_{1\text{eff}} = \left[\Omega' - \frac{g^2 \Omega' N_j}{8(\Omega^2 - \Omega'^2)} \right] S_z + \chi_{1\text{eff}} S_x^2,$$

$$H_{2\text{eff}} = \left[\Omega' + \frac{1}{2}g N_j - \frac{g^2 \Omega' N_j}{4(\Omega^2 - \Omega'^2)} \right] S_z + \chi_{2\text{eff}} S_z^2,$$

$$H_{3\text{eff}} = \left[\Omega' - g N_j - \frac{g^2 \Omega' N_j}{4(\Omega^2 - \Omega'^2)} \right] S_z + \chi_{3\text{eff}} S_z^2, \quad (\text{A15})$$

with effective interaction strength $\chi_{1\text{eff}} = g^2 \Omega N_j / [4(\Omega^2 - \Omega'^2)]$, $\chi_{2\text{eff}} = \chi_{3\text{eff}} = -g^2 N_j / [4(\Omega - \Omega')]$. For H_2 and H_3 , we have used the identity $S_x^2 + S_y^2 = S^2 - S_z^2 = s(s+1) - S_z^2$ and ignored the constant terms. The linear term $\propto S_z$ can be eliminated by choosing appropriate magnitudes of driving fields to make $f = 0$, then all three effective Hamiltonians are reduced to pure OAT Hamiltonians $H_{\text{eff}}^{\text{OAT}} = \chi_{\text{eff}} S_\mu^2$.

Appendix B: Generation of the effective TAT Hamiltonian with continuous driving

An effective Hamiltonian with the form $pS_x^2 + qS_y^2$ can be obtained by adding constant DC driving fields in cou-

pled spin systems, as shown in appendix A. If $p = -q$ or $p = 2q$ or $p = q/2$ is satisfied, the effective TAT interaction $\propto (S_i^2 - S_j^2)(i, j = x, y, z)$ can be obtained. Unfortunately, considering the condition of Eq. (A11), the tuning ranges of parameters p and q are not broad enough to directly obtain the effective TAT interaction. This imperfection can be overcome by adding an additional driving field. As suggested in Refs. [56, 58], we could transform an OAT Hamiltonian into an effective TAT Hamiltonian by using a pulsed or continuous driving. Here we provide a general scheme to transform any Hamiltonian of the form $pS_x^2 + qS_y^2$ into a pure effective TAT Hamiltonian with continuous driving.

If $(p - 2q)(2p - q) \geq 0$, we add a continuous AC field along z axis and get

$$H = pS_x^2 + qS_y^2 + AS_z \cos \omega t. \quad (\text{B1})$$

In the interaction picture defined by

$$|\psi_{\text{I}}(t)\rangle = U_{\text{I}}(t) |\psi(t)\rangle, \quad (\text{B2})$$

$$H_{\text{I}} = U_{\text{I}}^\dagger(t) H_0 U_{\text{I}}(t),$$

where

$$H_0 = pS_x^2 + qS_y^2,$$

$$U_{\text{I}} = \exp\left(-i \int_0^t AS_z \cos \omega \tau d\tau\right) \quad (\text{B3})$$

$$= \exp\left(-i \frac{A}{\omega} S_z \sin \omega t\right),$$

we can obtain

$$H_{\text{I}} = \left[\frac{p+q}{2} - \frac{q-p}{2} \cos\left(\frac{2A}{\omega} \sin \omega t\right) \right] S_x^2 + \left[\frac{p+q}{2} + \frac{q-p}{2} \cos\left(\frac{2A}{\omega} \sin \omega t\right) \right] S_y^2$$

$$+ \frac{q-p}{2} \sin\left(\frac{2A}{\omega} \sin \omega t\right) (S_x S_y + S_y S_x), \quad (\text{B4})$$

where we have used $e^{i\phi S_z} S_x e^{-i\phi S_z} = S_x \cos \phi - S_y \sin \phi$ and $e^{i\phi S_z} S_y e^{-i\phi S_z} = S_y \cos \phi + S_x \sin \phi$.

Now we apply the Jacobi-Anger expansion $e^{iz \sin \theta} = \sum_{n=-\infty}^{\infty} J_n(z) e^{in\theta}$, where $J_n(z)$ is the n th Bessel function

of the first kind, and only keep the zero-order term with $n = 0$ (rotating wave approximation), the Hamiltonian becomes

$$H_{\text{I}} \approx \left[\frac{p+q}{2} - \frac{q-p}{2} J_0\left(\frac{2A}{\omega}\right) \right] S_x^2 + \left[\frac{p+q}{2} + \frac{q-p}{2} J_0\left(\frac{2A}{\omega}\right) \right] S_y^2. \quad (\text{B5})$$

This approximation requires $\omega \ll N_s(p+q)$.

The Hamiltonian H_I can be rewritten by adding a

constant term $-[(p+q)/2 - (q-p)J_0(2A/\omega)/2]S^2$ or $-[(p+q)/2 + (q-p)J_0(2A/\omega)/2]S^2$, which leads to

$$\begin{aligned} H_I^{(1)} &= (q-p)J_0\left(\frac{2A}{\omega}\right)S_y^2 - \left[\frac{p+q}{2} - \frac{q-p}{2}J_0\left(\frac{2A}{\omega}\right)\right]S_z^2, \\ H_I^{(2)} &= (p-q)J_0\left(\frac{2A}{\omega}\right)S_x^2 - \left[\frac{p+q}{2} + \frac{q-p}{2}J_0\left(\frac{2A}{\omega}\right)\right]S_z^2. \end{aligned} \quad (\text{B6})$$

The effective TAT Hamiltonian is obtained when setting $J_0(2A/\omega) = \pm(p+q)/[3(q-p)]$ ("+" for (1) and "-" for (2)), that is,

$$\begin{aligned} H_{\text{eff}}^{(1)} &= \frac{p+q}{3}(S_y^2 - S_z^2), \\ H_{\text{eff}}^{(2)} &= \frac{p+q}{3}(S_x^2 - S_z^2). \end{aligned} \quad (\text{B7})$$

If $(p-2q)(2p-q) < 0$, we may add a continuous AC field along y axis. The Hamiltonian is equivalent to

$$H' = -qS_z^2 + (p-q)S_x^2 + AS_y \cos \omega t. \quad (\text{B8})$$

With similar analysis, we find the effective TAT Hamiltonian is obtained when $J_0(2A/\omega) = \pm(p-2q)/3p$, and the result is

$$\begin{aligned} H'_{\text{eff}}{}^{(1)} &= \frac{p-2q}{3}(S_x^2 - S_y^2), \\ H'_{\text{eff}}{}^{(2)} &= \frac{p-2q}{3}(S_z^2 - S_y^2). \end{aligned} \quad (\text{B9})$$

- [1] M. Kitagawa and M. Ueda, *Phys. Rev. A* **47**, 5138 (1993).
[2] D. J. Wineland, J. J. Bollinger, W. M. Itano, F. L. Moore, and D. J. Heinzen, *Phys. Rev. A* **46**, R6797 (1992).
[3] D. J. Wineland, J. J. Bollinger, W. M. Itano, and D. J. Heinzen, *Phys. Rev. A* **50**, 67 (1994).
[4] J. Ma, X. Wang, C. P. Sun, and F. Nori, *Phys. Rep.* **509**, 89 (2011).
[5] J. G. Bohnet, K. C. Cox, M. A. Norcia, J. M. Weiner, Z. Chen, and J. K. Thompson, *Nat. Photonics* **8**, 731 (2014).
[6] O. Hosten, R. Krishnakumar, N. J. Engelsens, and M. A. Kasevich, *Science* **352**, 1552 (2016).
[7] O. Hosten, N. J. Engelsens, R. Krishnakumar, and M. A. Kasevich, *Nature* **529**, 505 (2016).
[8] X.-Y. Luo, Y.-Q. Zou, L.-N. Wu, Q. Liu, M.-F. Han, M. K. Tey, and L. You, *Science* **355**, 620 (2017).
[9] H. Bao, J. Duan, S. Jin, X. Lu, P. Li, W. Qu, M. Wang, I. Novikova, E. E. Mikhailov, K.-F. Zhao, K. Mølmer, H. Shen, and Y. Xiao, *Nature* **581**, 159 (2020).
[10] A. André, A. S. Sørensen, and M. D. Lukin, *Phys. Rev. Lett.* **92**, 230801 (2004).
[11] D. Meiser, J. Ye, and M. J. Holland, *New J. Phys.* **10**, 073014 (2008).
[12] E. S. Polzik, *Nature* **453**, 45 (2008).
[13] C. Gross, T. Zibold, E. Nicklas, J. Estève, and M. K. Oberthaler, *Nature* **464**, 1165 (2010).
[14] M. F. Riedel, P. Böhi, Y. Li, T. W. Hänsch Signnsch, A. Sinatra, and P. Treutlein, *Nature* **464**, 1170 (2010).
[15] I. D. Leroux, M. H. Schleier-Smith, and V. Vuletić, *Phys. Rev. Lett.* **104**, 073602 (2010).
[16] R. J. Sewell, M. Koschorreck, M. Napolitano, B. Dubost, N. Behbood, and M. W. Mitchell, *Phys. Rev. Lett.* **109**, 253605 (2012).
[17] K. C. Cox, G. P. Greve, J. M. Weiner, and J. K. Thompson, *Phys. Rev. Lett.* **116**, 093602 (2016).
[18] L. Pezzè, A. Smerzi, M. K. Oberthaler, R. Schmied, and P. Treutlein, *Rev. Mod. Phys.* **90**, 035005 (2018).
[19] R. Kaubruegger, P. Silvi, C. Kokail, R. van Bijnen, A. M. Rey, J. Ye, A. M. Kaufman, and P. Zoller, *Phys. Rev. Lett.* **123**, 260505 (2019).
[20] E. Pedrozo-Peñañafiel, S. Colombo, C. Shu, A. F. Adiyatullin, Z. Li, E. Mendez, B. Braverman, A. Kawasaki, D. Akamatsu, Y. Xiao, and V. Vuletić, *Nature* **588**, 414 (2020).
[21] S. S. Szigeti, S. P. Nolan, J. D. Close, and S. A. Haine, *Phys. Rev. Lett.* **125**, 100402 (2020).
[22] A. Sørensen, L.-M. Duan, J. I. Cirac, and P. Zoller, *Nature* **409**, 63 (2001).
[23] A. S. Sørensen and K. Mølmer, *Phys. Rev. Lett.* **86**, 4431 (2001).
[24] X. Wang and B. C. Sanders, *Phys. Rev. A* **68**, 012101 (2003).
[25] J. K. Korbicz, J. I. Cirac, and M. Lewenstein, *Phys. Rev. Lett.* **95**, 120502 (2005).
[26] J. K. Korbicz, O. Gühne, M. Lewenstein, H. Häffner, C. F. Roos, and R. Blatt, *Phys. Rev. A* **74**, 052319 (2006).
[27] J. Estève, C. Gross, A. Weller, S. Giovanazzi, and M. K. Oberthaler, *Nature* **455**, 1216 (2008).
[28] G. Tóth, C. Knapp, O. Gühne, and H. J. Briegel, *Phys. Rev. A* **79**, 042334 (2009).
[29] P. Hyllus, L. Pezzè, A. Smerzi, and G. Tóth, *Phys. Rev. A* **86**, 012337 (2012).
[30] G. Tóth and I. Apellaniz, *J. Phys. A Math. Theor.* **47**, 424006 (2014).
[31] J. G. Bohnet, B. C. Sawyer, J. W. Britton, M. L. Wall, A. M. Rey, M. Foss-Feig, and J. J. Bollinger, *Science* **352**, 1297 (2016).

- [32] Z. Ren, W. Li, A. Smerzi, and M. Gessner, *Phys. Rev. Lett.* **126**, 080502 (2021).
- [33] J. Feng, E. O. Ilo-Okeke, A. N. Pyrkov, A. Askitopoulos, and T. Byrnes, *Phys. Rev. A* **104**, 013318 (2021).
- [34] J. Hald, J. L. Sørensen, C. Schori, and E. S. Polzik, *Phys. Rev. Lett.* **83**, 1319 (1999).
- [35] M. Takeuchi, S. Ichihara, T. Takano, M. Kumakura, T. Yabuzaki, and Y. Takahashi, *Phys. Rev. Lett.* **94**, 023003 (2005).
- [36] M. H. Schleier-Smith, I. D. Leroux, and V. Vuletić, *Phys. Rev. A* **81**, 021804(R) (2010).
- [37] K. Hammerer, A. S. Sørensen, and E. S. Polzik, *Rev. Mod. Phys.* **82**, 1041 (2010).
- [38] L. Yu, J. Fan, S. Zhu, G. Chen, S. Jia, and F. Nori, *Phys. Rev. A* **89**, 023838 (2014).
- [39] Y.-L. Zhang, C.-L. Zou, X.-B. Zou, L. Jiang, and G.-C. Guo, *Phys. Rev. A* **91**, 033625 (2015).
- [40] Y.-C. Zhang, X.-F. Zhou, X. Zhou, G.-C. Guo, and Z.-W. Zhou, *Phys. Rev. Lett.* **118**, 083604 (2017).
- [41] W. Qin, Y.-H. Chen, X. Wang, A. Miranowicz, and F. Nori, *Nanophotonics* **9**, 4853 (2020).
- [42] P. Groszkowski, H.-K. Lau, C. Leroux, L. C. G. Govia, and A. A. Clerk, *Phys. Rev. Lett.* **125**, 203601 (2020).
- [43] C. Orzel, A. K. Tuchman, M. L. Fenselau, M. Yasuda, and M. A. Kasevich, *Science* **291**, 2386 (2001).
- [44] M. Fadel, T. Zibold, B. Décamps, and P. Treutlein, *Science* **360**, 409 (2018).
- [45] A. Kuzmich, K. Mølmer, and E. S. Polzik, *Phys. Rev. Lett.* **79**, 4782 (1997).
- [46] L. Vernac, M. Pinard, and E. Giacobino, *Phys. Rev. A* **62**, 063812 (2000).
- [47] M. Fleischhauer and S. Gong, *Phys. Rev. Lett.* **88**, 070404 (2002).
- [48] M. A. Norcia, R. J. Lewis-Swan, J. R. K. Cline, B. Zhu, A. M. Rey, and J. K. Thompson, *Science* **361**, 259 (2018).
- [49] R. J. Lewis-Swan, M. A. Norcia, J. R. K. Cline, J. K. Thompson, and A. M. Rey, *Phys. Rev. Lett.* **121**, 070403 (2018).
- [50] A. Kuzmich, L. Mandel, and N. P. Bigelow, *Phys. Rev. Lett.* **85**, 1594 (2000).
- [51] J. Appel, P. J. Windpassinger, D. Oblak, U. B. Hoff, N. Kjærgaard, and E. S. Polzik, *Proc. Natl. Acad. Sci.* **106**, 10960 LP (2009).
- [52] Z. Chen, J. G. Bohnet, S. R. Sankar, J. Dai, and J. K. Thompson, *Phys. Rev. Lett.* **106**, 133601 (2011).
- [53] M. A. C. Rossi, F. Albarelli, D. Tamascelli, and M. G. Genoni, *Phys. Rev. Lett.* **125**, 200505 (2020).
- [54] M. Kritsotakis, J. A. Dunningham, and S. A. Haine, *Phys. Rev. A* **103**, 023318 (2021).
- [55] A. Kuzmich, N. P. Bigelow, and L. Mandel, *Europhys. Lett.* **42**, 481 (1998).
- [56] Y. C. Liu, Z. F. Xu, G. R. Jin, and L. You, *Phys. Rev. Lett.* **107**, 013601 (2011).
- [57] J. Y. Zhang, X. F. Zhou, G. C. Guo, and Z. W. Zhou, *Phys. Rev. A* **90**, 013604 (2014).
- [58] W. Huang, Y.-L. Zhang, C.-L. Zou, X.-B. Zou, and G.-C. Guo, *Phys. Rev. A* **91**, 043642 (2015).
- [59] C. Shen and L.-M. Duan, *Phys. Rev. A* **87**, 051801(R) (2013).
- [60] J. Hu, W. Chen, Z. Vendeiro, A. Urvoy, B. Braverman, and V. Vuletić, *Phys. Rev. A* **96**, 050301 (2017).
- [61] F. Chen, J.-J. Chen, L.-N. Wu, Y.-C. Liu, and L. You, *Phys. Rev. A* **100**, 041801(R) (2019).
- [62] C. Figgatt, A. Ostrander, N. M. Linke, K. A. Landsman, D. Zhu, D. Maslov, and C. Monroe, *Nature* **572**, 368 (2019).
- [63] Y. Lu, S. Zhang, K. Zhang, W. Chen, Y. Shen, J. Zhang, J.-N. Zhang, and K. Kim, *Nature* **572**, 363 (2019).
- [64] C. Song, K. Xu, W. Liu, C.-p. Yang, S.-B. Zheng, H. Deng, Q. Xie, K. Huang, Q. Guo, L. Zhang, P. Zhang, D. Xu, D. Zheng, X. Zhu, H. Wang, Y.-A. Chen, C.-Y. Lu, S. Han, and J.-W. Pan, *Phys. Rev. Lett.* **119**, 180511 (2017).
- [65] C. Song, K. Xu, H. Li, Y.-R. Zhang, X. Zhang, W. Liu, Q. Guo, Z. Wang, W. Ren, J. Hao, H. Feng, H. Fan, D. Zheng, D.-W. Wang, H. Wang, and S.-Y. Zhu, *Science* **365**, 574 (2019).
- [66] K. Xu, Z.-H. Sun, W. Liu, Y.-R. Zhang, H. Li, H. Dong, W. Ren, P. Zhang, F. Nori, D. Zheng, H. Fan, and H. Wang, *Sci. Adv.* **6**, eaba4935 (2020).
- [67] K. Helmerson and L. You, *Phys. Rev. Lett.* **87**, 170402 (2001).
- [68] M. Wang, W. Qu, P. Li, H. Bao, V. Vuletić, and Y. Xiao, *Phys. Rev. A* **96**, 013823 (2017).
- [69] J. Borregaard, E. J. Davis, G. S. Bentsen, M. H. Schleier-Smith, and A. S. Sørensen, *New Journal of Physics* **19**, 093021 (2017).
- [70] V. Macrì, F. Nori, S. Savasta, and D. Zueco, *Phys. Rev. A* **101**, 053818 (2020).
- [71] P. Cappellaro and M. D. Lukin, *Phys. Rev. A* **80**, 032311 (2009).
- [72] K. I. O. Ben 'Attar, D. Farfurnik, and N. Bar-Gill, *Phys. Rev. Research* **2**, 013061 (2020).
- [73] J. Choi, H. Zhou, H. S. Knowles, R. Landig, S. Choi, and M. D. Lukin, *Phys. Rev. X* **10**, 031002 (2020).
- [74] H. Zhou, J. Choi, S. Choi, R. Landig, A. M. Douglas, J. Isoya, F. Jelezko, S. Onoda, H. Sumiya, P. Cappellaro, H. S. Knowles, H. Park, and M. D. Lukin, *Phys. Rev. X* **10**, 031003 (2020).
- [75] L.-G. Huang, F. Chen, X. Li, Y. Li, R. Lü, and Y.-C. Liu, *npj Quantum Inf.* **7**, 168 (2021).
- [76] W. Muessel, H. Strobel, D. Linnemann, T. Zibold, B. Juliá-Díaz, and M. K. Oberthaler, *Phys. Rev. A* **92**, 023603 (2015).
- [77] S. A. Haine and J. J. Hope, *Phys. Rev. Lett.* **124**, 060402 (2020).
- [78] H. Fröhlich, *Phys. Rev.* **79**, 845 (1950).
- [79] S. Nakajima, *Advances in Physics* **4**, 363 (1955).
- [80] E. Davis, G. Bentsen, and M. Schleier-Smith, *Phys. Rev. Lett.* **116**, 053601 (2016).
- [81] S. P. Nolan, S. S. Szigeti, and S. A. Haine, *Phys. Rev. Lett.* **119**, 193601 (2017).
- [82] G.-R. Jin, Y.-C. Liu, and W.-M. Liu, *New J. Phys.* **11**, 73049 (2009).